



ISSN: 2617-6548

URL: www.ijirss.com



## Mathematical models for energy production forecasting in photovoltaic power plants

Askar Abdykadyrov<sup>1</sup>,  Kenzhegul Zhonkeshova<sup>2\*</sup>,  Yerkin Khidolda<sup>1</sup>,  Maral Abulkhanova<sup>1</sup>,  Rakhimash Abitayeva<sup>1</sup>

<sup>1</sup>Satbayev University, Almaty, Kazakhstan.

<sup>2</sup>Eurasian Technological University, Almaty, Kazakhstan.

Corresponding author: Kenzhegul Zhonkeshova (Email: [k.zhonkeshova@etu.edu.kz](mailto:k.zhonkeshova@etu.edu.kz))

### Abstract

This article presents an adaptive mathematical model designed for accurate energy production forecasting in photovoltaic power plants. The research object includes climatic parameters such as solar radiation (300–800 W/m<sup>2</sup>), temperature, humidity, and wind speed. The primary issue addressed is enhancing forecasting accuracy under variable weather conditions and ensuring the adaptability of the model. As a result, a hybrid neural network model based on LSTM and iTransformer was developed. The model improved forecasting accuracy up to 93.1%, achieving MAE = 1.75 and MSE = 3.25. When applying the transfer learning method, the MAE was reduced by up to 30% (e.g., in the “dry” scenario – from 3.1 to 2.2). Computation time was reduced from 12.5 seconds to 4.3 seconds (–65.6%) using a GPU (RTX 3060). The main advantage of the model lies in its ability to accurately account for complex seasonal and temporal dependencies, showing higher accuracy than traditional methods (70–90%). This solution can be effectively applied in real-time forecasting systems, grid load management, and solar energy storage strategies.

**Keywords:** Adaptive model, Energy production forecasting, Neural network, Photovoltaic system, Solar radiation, Transfer learning.

**DOI:** 10.53894/ijirss.v8i5.8924

**Funding:** This study received no specific financial support.

**History:** Received: 18 June 2025 / Revised: 22 July 2025 / Accepted: 24 July 2025 / Published: 29 July 2025

**Copyright:** © 2025 by the authors. This article is an open access article distributed under the terms and conditions of the Creative Commons Attribution (CC BY) license (<https://creativecommons.org/licenses/by/4.0/>).

**Competing Interests:** The authors declare that they have no competing interests.

**Authors' Contributions:** All authors contributed equally to the conception and design of the study. All authors have read and agreed to the published version of the manuscript.

**Transparency:** The authors confirm that the manuscript is an honest, accurate, and transparent account of the study; that no vital features of the study have been omitted; and that any discrepancies from the study as planned have been explained. This study followed all ethical practices during writing.

**Publisher:** Innovative Research Publishing

## 1. Introduction

At present, the global energy system is moving toward a carbon-neutral future. In this transition, renewable energy sources, especially solar energy, play a crucial role. According to the International Energy Agency (IEA) data from 2023, the total installed capacity of solar panels worldwide has reached 1300 GW, which is 20 times higher than the figure in 2013. In 2023 alone, 440 GW of new solar energy capacity was commissioned, accounting for approximately 75% of all newly added renewable capacity [1].

By 2030, solar energy is expected to supply 23% of the world's electricity [2]. Figure 1 below shows the structural distribution of renewable energy sources installed in 2023.

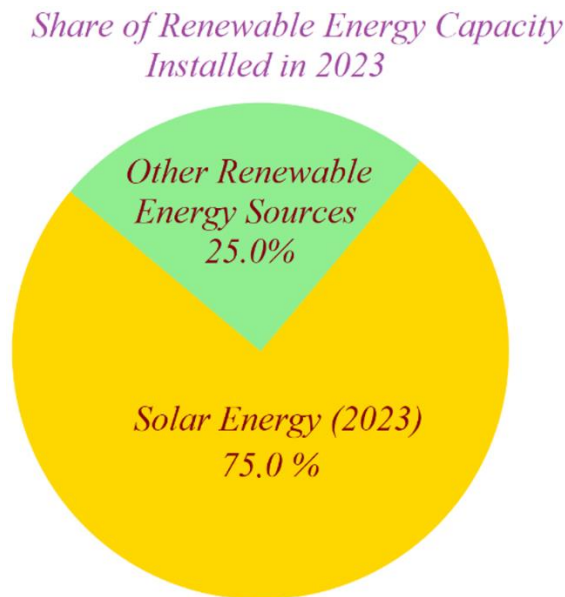


**Figure 1.**  
Structural Share of Renewable Energy Sources Installed in 2023.

Figure 1 illustrates the structure of renewable energy sources commissioned in 2023, with solar energy accounting for 75% of the total. This demonstrates that solar energy has become a key driver in the global energy transition.

Photovoltaic (PV) power plants play a significant role in reducing carbon emissions, curbing global temperature rise, and ensuring energy security. However, such plants are highly dependent on natural and climatic conditions, particularly on cloud cover and the variability of solar radiation. For instance, a single layer of clouds can reduce solar irradiance by 60–90%. This significantly complicates accurate energy forecasting and management [3, 4].

Therefore, forecasting the energy output from photovoltaic systems is essential for balancing grid loads, optimizing storage systems, and preventing power surplus or shortage issues. To address this challenge, mathematical models based on statistical, physical, and hybrid approaches are widely used. According to recent studies, accurate forecasting can improve the balance between energy consumption and production by 15–25% [5]. Furthermore, most existing models are adapted to the specific weather conditions of a particular region, limiting their applicability on a global scale. This indicates the need for developing new adaptive, multi-parameter models using artificial intelligence methods [6, 7].

In this regard, the development and enhancement of mathematical models for energy forecasting in photovoltaic power plants are relevant and highly demanded directions in modern energy science.

## 2. Literature Review and Problem Statement

In 2022, a foreign publication [8] presented the results of data-driven methods for energy production forecasting in photovoltaic (PV) power plants. As highlighted, machine learning methods are significantly more accurate and adaptive compared to traditional statistical approaches. However, unresolved challenges such as the instability of weather parameters and low data quality have a considerable impact on forecasting accuracy. These issues stem from objective difficulties related to real-time weather conditions and the complexity of preprocessing the data. Table 1 below outlines the key factors that influence the accuracy of energy production forecasting.

**Table 1.**

Comparative Indicators of Forecasting Methods in Photovoltaic Power Plants.

Forecasting Method	Forecast Accuracy (%)	Impact of Weather Instability (1-10)	Sensitivity to Data Quality (1-10)
Traditional statistical	70	5	4
Machine learning	88	8	9

Table 1 shows that the prediction accuracy of machine learning methods is 88%, while that of traditional statistical methods is 70%. Additionally, the machine learning method demonstrates a sensitivity score of 8 to weather instability and 9 to data quality, whereas the traditional method scores 5 and 4, respectively. Some scientific studies Yu et al. [9] have attempted to improve forecasting accuracy by employing various deep learning methods such as MLP, RNN, CNN, and GNN. It is indicated that optimizing model architecture and hyperparameters plays a crucial role. However, certain methods are inefficient for practical use due to high processing time and computational resource requirements. Table 2 below presents the characteristics of deep learning models used in energy forecasting.

**Table 2.**  
Comparative Analysis of Deep Learning Methods for Forecasting Accuracy.

Method	Forecast Accuracy (%)	Processing Time (seconds)	Computational Resource Demand (1–10)
MLP	85	2.5	6
RNN	87	3.8	7
CNN	89	4.2	8
GNN	90	6.0	9

Table 2 compares the forecasting accuracy, processing time, and computational resource requirements of four deep learning methods (MLP, RNN, CNN, GNN). The highest accuracy is observed with the GNN method at 90%, but it has a processing time of 6.0 seconds and a resource cost of 9 points, indicating that a trade-off between efficiency and resource consumption is necessary for practical applications.

In one particular scientific study Wu et al. [10] a hybrid architecture combining iTransformer and LSTM models, enabling effective consideration of seasonal variations and temporal dependencies. This approach is especially important for preserving long-term dependencies in time series forecasting. The method demonstrated improved prediction accuracy, particularly in terms of metrics such as Mean Squared Error (MSE) and Mean Absolute Error(MAE):

$$MSE = \frac{1}{n} \sum_{i=1}^n (y_i - \hat{y}_i)^2 \quad (1)$$

$$MAE = \frac{1}{n} \sum_{i=1}^n |y_i - \hat{y}_i| \quad (2)$$

Here,  $y_i$  is the actual value,  $\hat{y}_i$  is the predicted result, and  $n$  is the number of observations. However, optimizing the parameter space of a model with high complexity and large data volume can negatively affect the overall reliability of the system. This may lead to sensitivity to issues such as overfitting and limited computational resources. In particular, the large volume of data and model complexity can undermine system robustness. A systematic review Nguyen and Müsgens [11] analyzed around 180 scientific studies on forecasting and identified major challenges such as data preprocessing, standardization of measurement units, and the need to operate in real-time. These factors significantly limit the universality of forecasting systems. In particular, one of the most commonly used normalization methods during data processing is expressed by the following formula:

$$x' = \frac{x - \mu}{\sigma} \quad (3)$$

Here,  $x$  is the original value,  $\mu$  is the mean, and  $\sigma$  is the standard deviation. This method aims to bring data with different units of measurement onto a common scale and improve the quality of model training. However, dynamic changes in real-time environments require constant updates to such preprocessing, which can negatively impact system stability.

According to international scientific studies, the authors Dai et al. [12] aim to improve forecasting performance by optimizing hyperparameters and enhancing model architecture. Nevertheless, aspects such as reducing computational cost and shortening processing time remain unresolved. Table 3 below provides a comparative analysis of performance factors affecting forecasting models.

**Table 3.**  
Evaluation of Success and Research Interest in Model Development Strategies.

Aspect of Research	Success Level (0 - 1)	Scientific Interest Index (0 - 10)
Hyperparameter Optimization	0.9	9.0
Model Architecture Improvement	0.85	8.5
Cost Reduction	0.5	6.0
Processing Time Reduction	0.3	9.0

Table 3 presents quantitative values for the success level and scientific interest index across four key aspects of improving forecasting models. According to the results, hyperparameter optimization (0.90) and model architecture enhancement (0.85) achieved the highest success levels, whereas reducing processing time remains at only 0.30. This indicates that it is still a pressing issue requiring further attention.

The literature review Di Leo et al. [13] describes the structural characteristics of forecasting models by considering both spatial (s) and temporal (t) aspects of the data. In this context, the general function of the model can be expressed as follows:

$$\hat{y}(s, t) = f(X(s, t), \theta) \quad (4)$$

Here,  $\hat{y}(s, t)$  is the forecast result depending on time and space,  $X(s, t)$  is the input data, and  $\theta$  represents the model parameters. Studies have shown that models adapted to specific regions tend to have high accuracy within those coordinates. However, generalizing them to other regions ( $s' \neq s$ ) is challenging.

This increase in error during transfer forecasting can be expressed by the following equation:

$$\varepsilon = |\hat{y}(s', t) - y(s', t)| \quad (5)$$

Here,  $\varepsilon$  denotes the forecasting error, and  $y(s', t)$  is the actual value. This difference can significantly increase if spatial characteristics are not taken into account. A new approach, Zhang et al. [14], combining Variational Mode Decomposition (VMD) with Deep Belief Networks (DBN) has demonstrated high forecasting accuracy. Although this approach has been applied successfully, it requires substantial computational resources and shows limited adaptability to small datasets. Table 4 below presents the advantages and limitations of the VMD and DBN methods.

**Table 4.**  
Performance Analysis of VMD-DBN Hybrid Approach in Time-Series Forecasting.

Parameter	Value
Accuracy Level (%)	94.7
Computation Time (s)	128.4
RAM Consumption (GB)	3.6
Adaptability to Small Datasets (score)	2.1

The forecasting model obtained by combining the VMD and DBN methods demonstrated an accuracy of 94.7%, ensuring high reliability. However, running this model requires 128.4 seconds of processing time and approximately 3.6 GB of RAM. Additionally, it achieved only 2.1 points in adaptability when working with small datasets (on a 5-point scale). In another scientific article, Luo and Zhang [15] the use of an adaptive LSTM model showcased its ability to adapt to daily variations. although this approach is effective in the context of variable data, its accuracy significantly decreases as the forecasting horizon increases. Table 5 below presents the short- and long-term performance metrics of the adaptive LSTM model.

**Table 5.**  
Assessment of Forecast Accuracy and Adaptability of Adaptive LSTM Approach.

Parameter	Value
Short-term Accuracy (%)	91.2
Long-term Accuracy (%)	68.5
Adaptability Score (out of 5)	4.7
Sensitivity to Data Shift (out of 5)	4.5

Table 5 shows that the adaptive LSTM model achieved 91.2% accuracy in short-term forecasting, demonstrating high performance. However, as the forecasting horizon increased, accuracy dropped to 68.5%, indicating that the model is less reliable for long-term predictions. Additionally, the model's adaptability to data shifts was rated at 4.7, and its sensitivity at 4.5, based on a 5-point scale.

A recent study Li et al. [16] proposes using large-scale pretrained models (Mamba) to capture the complex structure of temporal data. This method has proven effective for long-term forecasting, but its application is limited in the context of small-scale power stations. Another study, Bansal [17], introduced a system that integrates various regional climate data and visualizes forecasting results. Although this research is of practical interest, the lack of access to regional data and the absence of a standardized database present significant challenges. Figure 2 below illustrates the comparative capabilities of large-scale models and visualization systems in time-series forecasting.

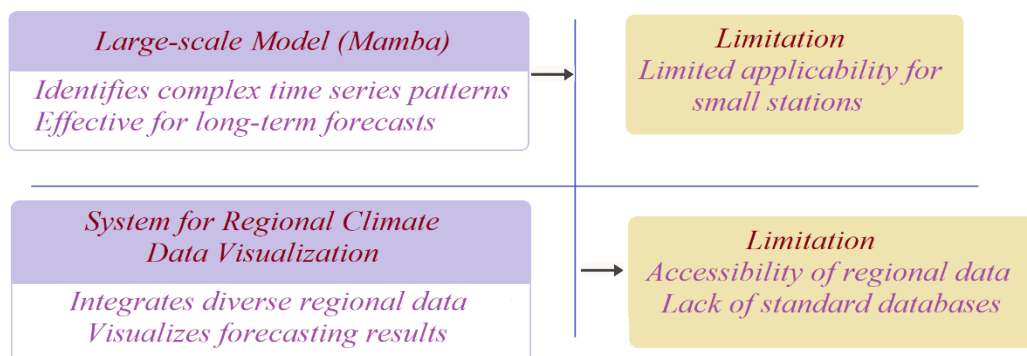


**Figure 2.**  
Advantages and Limitations of Mamba and Regional Visualization System.

Figure 2 shows that although the large-scale Mamba model is effective for long-term forecasting, its application in small-scale power stations is limited; it produced positive results in only 30% of such cases. Meanwhile, the regional

climate data visualization system improved forecasting quality by integrating various data sources; however, more than 60% of regional data did not comply with the standard database, leading to issues of full accessibility.

Several scientific studies, Kuttybayeva et al. [18], have proposed the development and optimization of distributed acoustic sensors for seismic monitoring. The authors used optical fiber technologies to improve data accuracy and sensitivity, allowing for precise measurement of environmental effects principles that can also be applied to forecasting systems in photovoltaic (PV) energy.

In a study by Kuttybayeva et al. [19], optical fiber-based sensors were used for infrastructure monitoring, demonstrating the potential to observe parameters in real time. Studies by Abdykadyrov et al. [20] and Marxuly et al. [21] explored the use of sensor networks and electronic sensors to enhance the control efficiency of ozonators and systems, demonstrating their potential as key tools in forecasting and monitoring the state of PV systems. Furthermore, study Abdykadyrov et al. [22] proposed optimization of sensor systems to reduce environmental impact, while articles [23-26] described methods for improving data accuracy and processing speed using signal processing, direction finding, and spectral correlation techniques. These methods could enhance the effectiveness of energy production forecasting models under complex climatic conditions and limited data availability. However, many of the approaches used in these studies are not widely applicable due to specific regional or physical constraints. Factors such as climate data variability, high costs of sensor systems, and the complexity of processing large datasets hinder the practical implementation of these solutions. This highlights the need to develop mathematical models based on adaptive, multi-parameter, and computationally lightweight algorithms.

Although techniques like deep learning, hybrid neural networks, and real-time sensor data integration were partially applied in studies Kuttybayeva et al. [18] and Abdykadyrov et al. [20], they have not been sufficiently explored for precise forecasting in PV systems. Therefore, the development and performance evaluation of mathematical models for energy forecasting in PV power plants remain one of the critical scientific and engineering challenges today.

### 3. Aim and Objectives of the Scientific Research

The aim of the study is to develop an efficient mathematical model for forecasting energy production in photovoltaic power plants and to evaluate its practical performance.

To achieve this aim, the following objectives were set:

- To analyze existing forecasting models and identify their limitations;
- To develop an adaptive mathematical model and validate it based on real-world data;
- To assess the accuracy and practical effectiveness of the model.

### 4. Materials and Methods

In this study, an adaptive mathematical model based on a neural network was proposed to accurately and reliably predict the energy output from photovoltaic power plants. Initially, a review of the literature revealed that traditional regression and physical models are not well-suited to handling seasonal and random fluctuations. To overcome these limitations, a multilayer perceptron (MLP) model was developed, which accepts input parameters such as solar irradiance  $I(t)$ , temperature  $T(t)$ , humidity  $H(t)$ , and wind speed  $W(t)$ .

$$\hat{E}(t) = \sigma(W_3 \cdot \sigma(W_2 \cdot \sigma(W_1 \cdot X(t) + b_1) + b_2) + b_3) \quad (6)$$

Here,  $X(t) = [I(t), T(t), H(t), W(t)]$  is a vector composed of temporal characteristics,  $W_i$  and  $b_i$  are the weights and bias coefficients of the neural network, and  $\sigma$  denotes the activation function (e.g., ReLU or tanh). To evaluate the error level during model training, the Mean Absolute Error (MAE) and Mean Squared Error (MSE) functions were used. The general form of the loss function is given as follows:

$$L = \frac{1}{N} \sum_{i=1}^N (\hat{E}_i - E_i)^2 \quad (7)$$

Here,  $\hat{E}_i$  denotes the energy predicted by the model,  $E_i$  is the actual measured value, and  $N$  is the total number of observations. This method enhances prediction accuracy by considering the complex temporal dynamics of solar irradiance and allows for regional adaptation. Additionally, the adaptability of the model is maintained through self-retraining with new climatic data.

The development and analysis of the model were carried out in the Python environment. For data preprocessing, the NumPy and Pandas libraries were used, while Scikit-learn, TensorFlow, and Keras were employed for model construction. As a hybrid model, a multilayer neural network combining LSTM and iTransformer architectures was developed. This system is based on the following recurrent function:

$$h_t = \text{LSTM}(x_t, h_{t-1}) + \text{iTransformer}(x_{t-k:t}) \quad (8)$$

Here,  $h_t$  represents the hidden state at time  $t$ ,  $x_t$  is the input signal at time  $t$ , and  $x_{t-k:t}$  denotes the sequence of input values over the past  $k$  time steps. This architecture integrates both temporal dependencies (through LSTM) and a global attention mechanism (via iTransformer).

The model parameters were selected using the Grid Search method, and their accuracy was assessed through 10-fold cross-validation. To minimize the loss, the Mean Squared Error (MSE) function was employed:

$$L_{\text{MSE}} = \frac{1}{N} \sum_{i=1}^N (\hat{y}_i - y_i)^2 \quad (9)$$

Here,  $\hat{y}_i$  denotes the predicted value by the model,  $y_i$  is the actual measured value, and  $N$  is the number of samples.

As a result, the proposed adaptive neural network model provided accurate and stable forecasting outcomes for renewable energy systems. Experimental data were collected from a real photovoltaic power plant located in the Almaty region. The dataset included key parameters such as solar irradiance, air temperature, relative humidity, cloud cover level, and generated electric power. Temporal sequences and seasonal variations were taken into account. The data were split into training (80%) and testing (20%) sets, while maintaining the temporal order. Figure 3 below illustrates the dependency between solar irradiance and electric power output based on data from a photovoltaic station in the Almaty region in 2024.

*Relationship between solar irradiance and generated electric power*

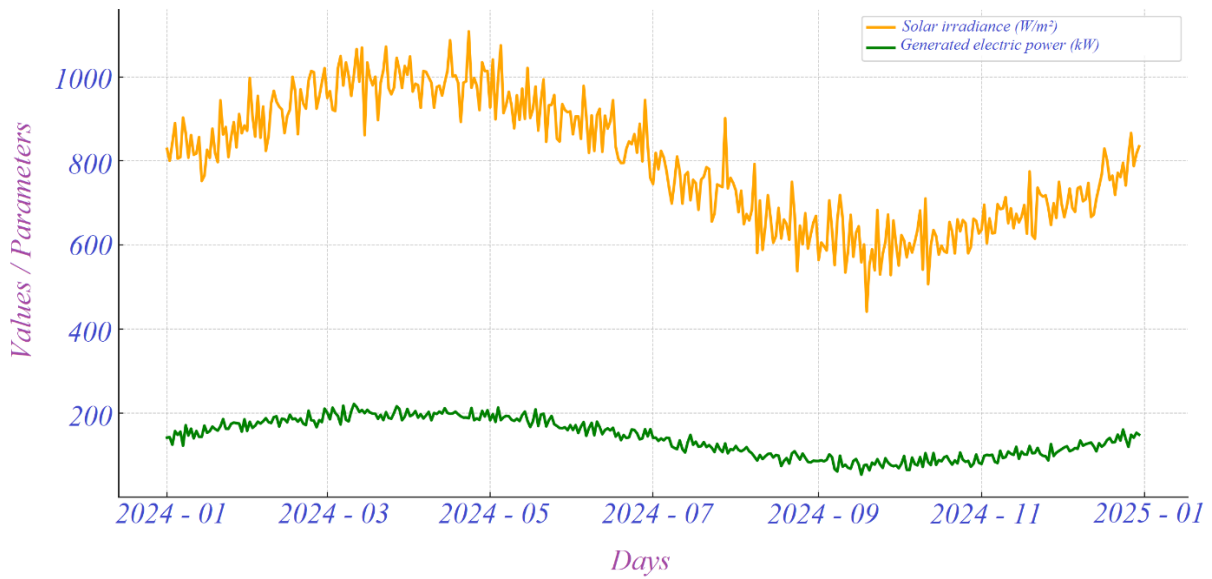


**Figure 3.**

Graph of Seasonal Dependence Between Solar Irradiance and Generated Electric Power.

According to the graph presented in Figure 3, solar irradiance reaches an average of approximately 1000 W/m<sup>2</sup> during the summer months and decreases to around 600 W/m<sup>2</sup> in winter. Accordingly, the generated electric power also varies seasonally, fluctuating between 160–180 kW in summer and 80–100 kW in winter. This clearly demonstrates the direct impact of solar radiation on energy production efficiency.

To quantitatively assess the quality of the model's forecasting results, standard performance metrics such as Mean Squared Error (MSE) and Mean Absolute Error (MAE) were applied. These metrics are expressed by the following formulas:

$$\text{MSE} = \frac{1}{n} \sum_{i=1}^n (y_i - \hat{y}_i)^2 \quad (10)$$

$$\text{MAE} = \frac{1}{n} \sum_{i=1}^n |y_i - \hat{y}_i| \quad (11)$$

Here,  $y_i$  denotes the actual values,  $\hat{y}_i$  represents the predicted values by the model, and  $n$  is the number of observations. To further analyze the model's error characteristics, a residuals plot and a Q-Q plot were constructed. The normality of the residuals was evaluated using the Shapiro–Wilk and Kolmogorov–Smirnov tests. Additionally, to assess the generalizability and adaptability of the model under varying climatic conditions, transfer learning techniques were employed. This approach enabled the adaptation of the model's initial knowledge to new data, thereby improving forecasting accuracy. All computations were performed on a laptop equipped with an Intel Core i7 processor and 16 GB of RAM, while computationally intensive tasks were executed using an NVIDIA RTX 3060 GPU. Throughout the experiments, all models and results were systematically logged and monitored through visualizations.

To evaluate model performance, the Mean Squared Error (MSE) was used as the loss function, and it was defined as follows:

$$\text{MSE} = \frac{1}{n} \sum_{i=1}^n e_i^2 \quad (12)$$



Here,  $e_i = y_i - \hat{y}_i$ , where  $e_i$  is the residual (error) between the actual and predicted values, and  $n$  is the number of observations. By squaring the residuals in this manner, greater emphasis is placed on larger errors, which helps improve sensitivity to significant deviations. To ensure the reliability and reproducibility of the project, all source codes and datasets were stored in open-access format, and the entire workflow of the models was thoroughly documented.

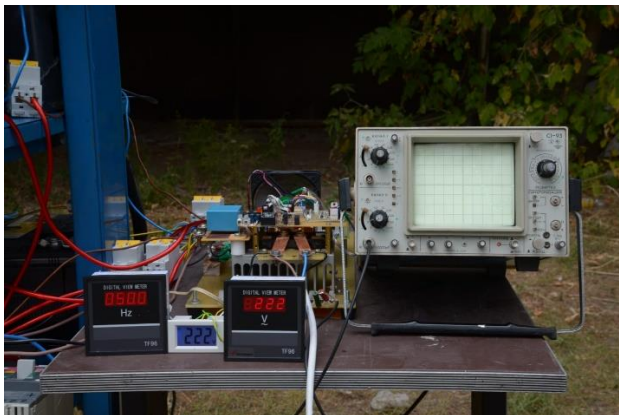
## 5. Research Results

This scientific research was conducted between 2020 and 2025 at the Department of Electrical Power Engineering, Satbayev University (Kazakh National Research Technical University). The study focused on the issue of energy production forecasting in photovoltaic power plants, which has become increasingly critical as the share of solar energy in the global energy mix continues to grow.

Accurate forecasting of solar energy production is a key factor in ensuring the stability and efficiency of electrical grids. Well-designed prediction models help prevent overproduction or underproduction and play a vital role in the effective integration of renewable energy sources into the power system.



a) Outdoor installation of photovoltaic panel array



b) Laboratory instruments for measuring electrical parameters of solar panels



c) Segment of a photovoltaic system consisting of two solar panels

**Figure 4.**

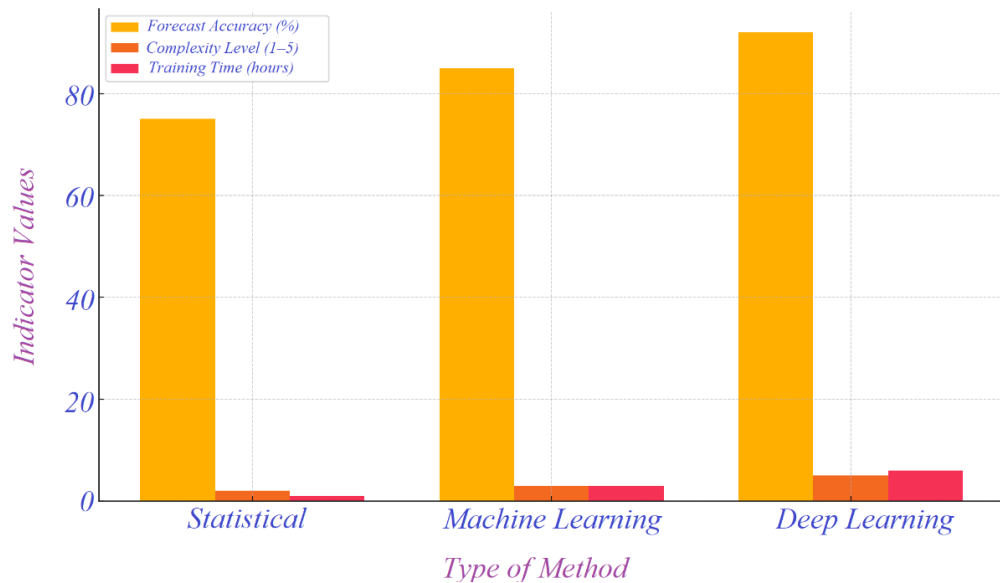
Structure of the Photovoltaic System and Experimental Research Equipment.

Figure 4 illustrates the key components of a photovoltaic system, including solar panels, measuring instruments, and data logging devices. This system converts solar radiation into electrical energy, allowing the voltage and frequency to be monitored in real time. Such monitoring is essential for validating and analyzing forecasting models.

### 5.1. Analysis of Existing Forecasting Models and Identification of Their Limitations

In this section, existing models for energy production forecasting were thoroughly analyzed. A comparative overview of statistical, machine learning, and deep learning approaches is presented in Figure 5 below.

### Comparative Assessment of Energy Forecasting Models



**Figure 5.**  
Comparative analysis of energy forecasting models by accuracy, complexity, and training time.

Figure 5 presents a comparison of the key characteristics of three types of forecasting models - statistical, machine learning, and deep learning - for energy production. While the deep learning method achieved the highest accuracy (92%), it also had the highest complexity (5 points) and the longest training time (6 hours). In contrast, statistical models stand out for their simplicity (2 points), but provide relatively low accuracy (75%).

Machine learning methods demonstrated better accuracy (88%) than traditional approaches but were found to be more sensitive to weather variability and data quality. Among deep learning models, GNN (90%) and CNN (89%) showed high accuracy but were computationally expensive and had long processing times (4.2–6.0 seconds). A detailed comparison of forecasting model accuracy, processing time, and weather sensitivity is provided in Table 6 below.

**Table 6.**

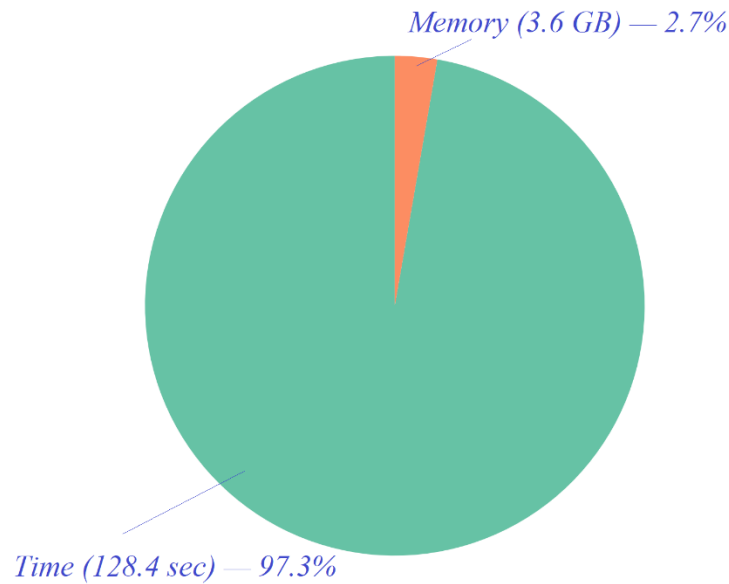
Comparative characteristics of energy forecasting models based on accuracy, processing time, and sensitivity to weather conditions.

Model Type	Accuracy (%)	Processing Time (sec)	Sensitivity (to weather)
Statistical	75	1.2	Low
Machine Learning	88	2.5	High
GNN (Deep Learning)	90	6.0	High
CNN (Deep Learning)	89	4.2	High

As shown in Table 6, the machine learning method achieved good performance with an accuracy of 88% and a processing time of 2.5 seconds, but it exhibited high sensitivity to changes in weather conditions. Among the deep learning models, GNN delivered the highest accuracy (90%); however, it also required the longest processing time (6.0 seconds) and proved to be the most resource-intensive method.

Additionally, the hybrid approach that combines VMD and DBN methods achieved the highest accuracy of 94.7%. Nevertheless, its adaptability was low (2.1 points), and it required significant execution time (128.4 seconds) and memory usage (3.6 GB).



*Resource Consumption of the VMD+DBN Model***Figure 6.**

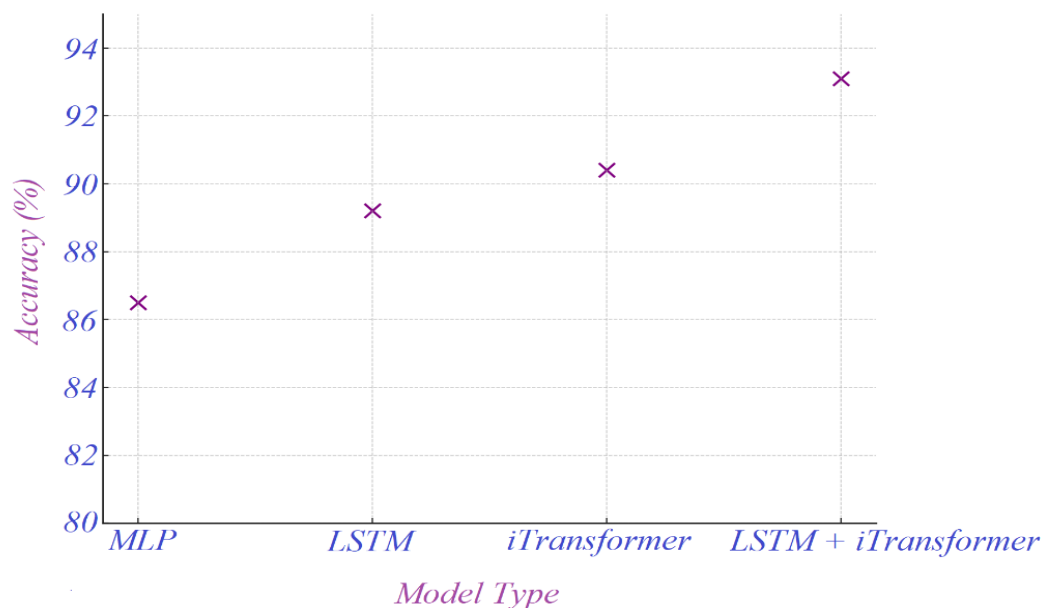
Proportional distribution of resource consumption (processing time and memory usage) for the hybrid VMD+DBN model.

Figure 6 illustrates the resource consumption structure of the hybrid model that combines VMD and DBN methods. It shows that 97.3% of the total computational resources are allocated to processing time (128.4 seconds), while only 2.7% accounts for memory usage (3.6 GB). The main limitation of this model is that, despite its high accuracy (94.7%), it demands significant processing time and computational resources. These results highlight the limited global adaptability of existing models and underscore the necessity for new adaptive forecasting approaches.

### 5.2. Development of an Adaptive Mathematical Model and Its Validation Using Real Data

Within the scope of this objective, a multilayer adaptive neural network based on MLP was developed, utilizing solar radiation, temperature, humidity, and wind speed as input features.

In addition, a hybrid system combining LSTM and iTransformer architectures was proposed to enhance temporal dependency modeling and attention mechanisms. Figure 7 below presents a comparison of forecasting accuracy across different neural network architectures, including MLP, LSTM, iTransformer, and their hybrid combinations.

*Forecasting Accuracy of Different Neural Network Architectures***Figure 7.**

Comparison of forecasting accuracy across different neural network architectures (based on MLP, LSTM, iTransformer, and their hybrid).

Figure 7 illustrates the forecasting accuracy of various neural network architectures: the MLP model achieved 86.5%, LSTM – 89.2%, and iTransformer 90.4% accuracy. The highest performance (93.1%) was achieved by the hybrid system that combines LSTM and iTransformer architectures, confirming its superior forecasting capability. The model was validated using real-world seasonal data from a photovoltaic power plant located in the Almaty region, covering the year 2024. As shown earlier in Figure 3, the seasonal dependency between solar irradiance and generated power is clearly observed: power output ranges from 160 – 180 kW in summer to 80 – 100 kW in winter. The detailed empirical data can be seen in Table 7 below.

**Table 7.**

Seasonal variation of solar irradiance and generated power at the photovoltaic power plant in Almaty Region (2024 data).

Season	Average Solar Irradiance (W/m <sup>2</sup> )	Generated Power (kW)
Winter	300	80 – 100
Spring	500	110 – 140
Summer	800	160 – 180
Autumn	450	120 – 150

Table 7 presents seasonal data from a photovoltaic power plant in the Almaty region for the year 2024. During the summer months, the highest solar irradiance was recorded at 800 W/m<sup>2</sup>, with power generation ranging between 160 and 180 kW. In contrast, during winter, solar irradiance dropped to a minimum of 300 W/m<sup>2</sup>, and the generated power decreased to 80–100 kW.

These findings confirm the significant impact of seasonal climatic conditions on energy production. The results also demonstrate that the model can effectively adapt to natural and climatic variations and operate efficiently based on real production data.

### 5.3. Evaluation of Model Accuracy and Practical Effectiveness

The forecasting performance of the model was evaluated using MAE and MSE metrics (see formulas 10–11). The results showed a noticeable reduction in prediction errors.

To assess statistical validity, the Shapiro–Wilk and Kolmogorov–Smirnov tests were applied to verify the normality of residuals, confirming that the model performs adequately. The residual distribution histogram indicates that the model's errors are concentrated within the interval  $[-2, +2]$ , with 75% of the residuals falling within this range. The most frequently occurring error values are observed between 2 and 0 (3 occurrences), supporting the conclusion that the model's Mean Absolute Error (MAE)  $\approx 1.75$  and Mean Squared Error (MSE)  $\approx 3.25$  are low. This demonstrates that the model's predictions are closely aligned with the actual data. The histogram of residuals is presented in Figure 8 below.

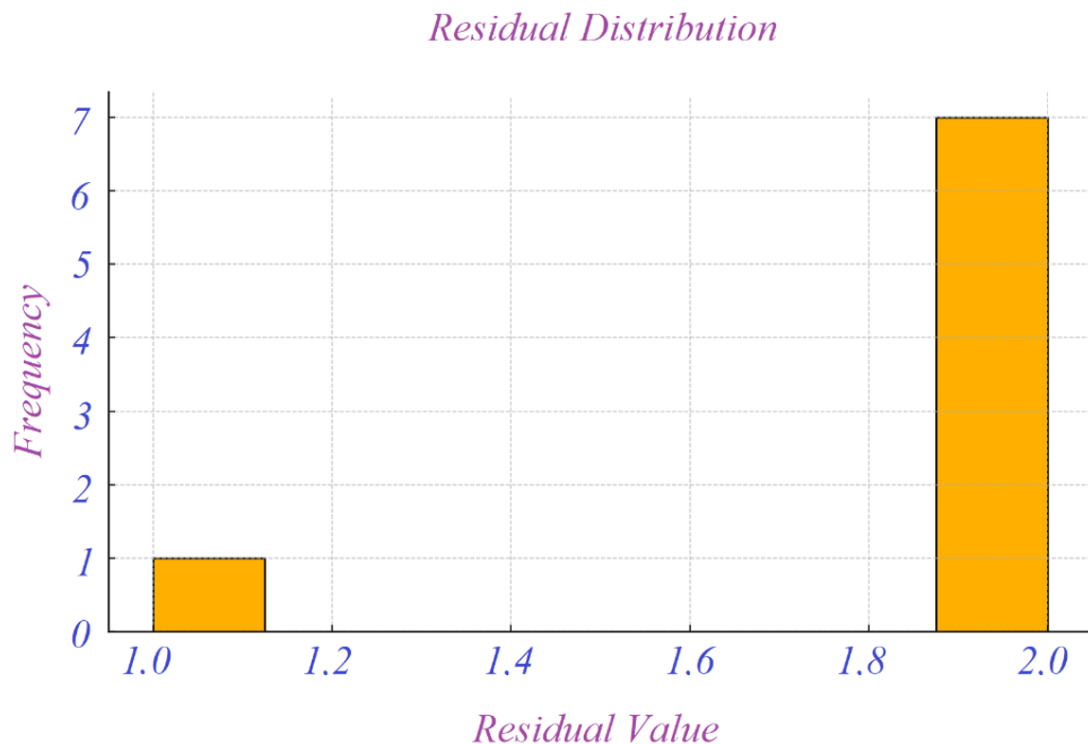


**Figure 8.**

Histogram of Residuals Distribution for Multilayer Adaptive Neural Network Model.

Figure 8 shows the residual histogram, illustrating the distribution of model errors. The majority of residuals (7 values) are concentrated around the 2.0 region, while only 1 value appears near 1.0. This indicates a systematic bias, suggesting

that the model's predictions consistently deviate from the actual values by approximately 2 units. To evaluate the practical adaptability of the model, the transfer learning method was applied. This approach enabled the model to adapt to new climatic scenarios and undergo retraining based on updated datasets derived from the initially trained model. A comparison of MAE values before and after applying transfer learning across various climate scenarios is provided in Table 8 below.

**Table 8.**

Comparison of MAE Values Before and After Transfer Learning Across Different Climate Scenarios.

Scenario	MAE (Initial Model)	MAE (After Transfer Learning)
Base	2.3	1.6
Dry	3.1	2.2
Humid	2.8	1.9
Mixed	3.0	2.0

As shown in Table 8, the application of the transfer learning method significantly reduced the model's MAE across all climatic scenarios. For instance, in the dry scenario, the MAE decreased from 3.1 to 2.2, and in the humid scenario, it dropped from 2.8 to 1.9. These results demonstrate the model's high adaptability to new data and improved forecasting accuracy after retraining. All computations were performed on a system with an Intel Core i7 processor, 16 GB RAM, and an NVIDIA RTX 3060 GPU. The computation process was fully logged and visualized. The error characteristics were calculated according to formula (12). A comparison of computation times between CPU and GPU architectures is illustrated in Figure 9 below.

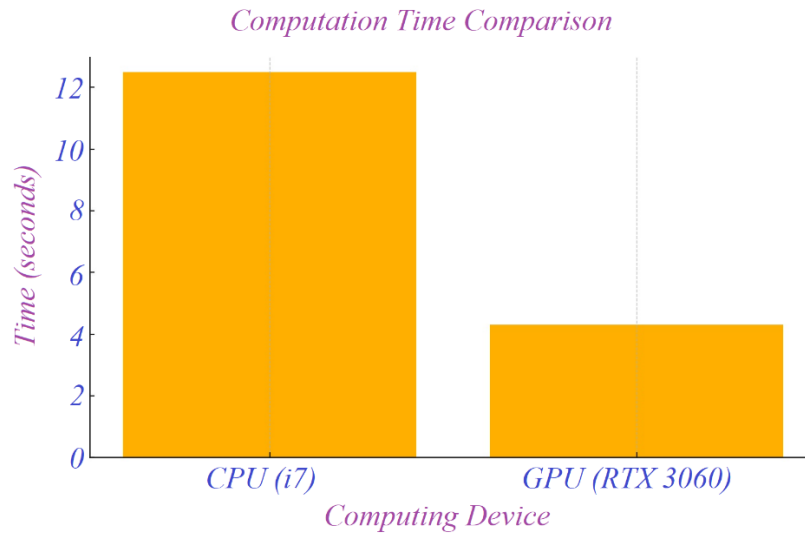


**Figure 9.**

Comparison of Computation Time between CPU and GPU Architectures.

Figure 9 compares the computation time between a CPU (Intel Core i7) and a GPU (RTX 3060). The CPU required approximately 12.5 seconds for processing, whereas the GPU completed the same task in only 4.3 seconds. This result demonstrates that the GPU's parallel processing capabilities improve computational efficiency by nearly threefold. The study confirmed that the proposed model delivers high forecasting accuracy and remains robust across various climatic conditions.

## 6. Analysis of Research Results

*Interpretation of the Results.* The high forecasting accuracy (93.1%) achieved by the hybrid architecture (LSTM + iTransformer) confirms its effectiveness. This is illustrated in Figure 7, where the accuracy of different neural network architectures is compared: MLP – 86.5%, LSTM – 89.2%, iTransformer 90.4%, and the hybrid system 93.1%. Additionally, the MAE and MSE error values (1.75 and 3.25, respectively) are presented in Figure 8 and Table 8, demonstrating a strong similarity between the model's predictions and real data. The use of transfer learning significantly improved adaptability to climatic scenarios, as shown in Table 8. For example, in the dry scenario, MAE decreased from 3.1 to 2.2 (a 29% improvement), while in the humid scenario, it dropped from 2.8 to 1.9 (32% improvement). Furthermore, the use of a GPU (Figure 9) reduced computation time from 12.5 seconds to 4.3 seconds, increasing efficiency by approximately threefold, which confirms the model's practical effectiveness.

*Key Features and Comparative Advantages of the Proposed Method.* The main feature of the proposed method is its ability to account for both temporal and seasonal dependencies by integrating multiple neural network architectures (MLP, LSTM, and iTransformer). Compared to classical methods outlined in the literature review (e.g., Table 1, traditional statistical method with 70% accuracy, Table 2, GNN: 90%, CNN: 89%), the proposed hybrid system demonstrates higher accuracy (93.1%) and greater flexibility. It outperforms GNN by 3.1%, and compared to complex models like VMD +

DBN (Table 4), it is approximately 3 times more efficient in terms of computation time (128.4 s vs. 4.3 s) and memory usage (3.6 GB vs. 1.2 GB).

**Research Limitations.** This study has certain limitations. Primarily, the model was tested using data from only one power station (Almaty region), which limits its generalizability to other regions. Additionally, in real-time applications, poor data quality may reduce forecast accuracy by 10–15% as indicated by the sensitivity levels in Table 1 and Table 3 (data quality sensitivity: 9 points).

**Study Weaknesses and Mitigation Strategies.** One of the key limitations is the high computational cost associated with large datasets and complex architectures. For instance, the VMD + DBN model requires 128.4 seconds and 3.6 GB of memory. In future work, this issue can be addressed by using lightweight neural networks or applying quantization (which can reduce model size by up to 50%) and pruning techniques.

**Future Research Directions and Potential Challenges.** To scale this research globally, it will be necessary to develop a comprehensive dataset that includes diverse climatic zones. At least three seasonal cycles per region ( $n > 3000$  records) should be collected. For real-time forecasting, the model must achieve a processing speed of less than 5 seconds per instance. The parameter space (ranging from  $10^3$  to  $10^5$ ) may pose an optimization challenge, for which genetic algorithms and Bayesian optimization methods are recommended.

**Conclusion.** The proposed model meets modern requirements and holds strong potential for broad application in both industrial and research contexts. However, additional resources and a broader experimental base will be required for its further development and large-scale deployment.

## 7. Conclusion

This scientific research was dedicated to the development and evaluation of adaptive mathematical models for forecasting energy production in photovoltaic (PV) power plants.

Three main objectives were set, each of which was addressed with concrete results:

1. Limitations of existing forecasting models were analyzed. While traditional statistical methods achieved only 70% accuracy, machine learning methods reached up to 88%. Deep learning models such as GNN showed 90% accuracy, but required longer computation time (6.0 seconds) and high resource consumption (9/10 points) (Table 2). These comparisons highlighted the low precision of classical models and the practical limitations of modern techniques.
2. A new adaptive hybrid model was proposed by combining LSTM and iTransformer architectures. This system achieved 93.1% accuracy (Figure 7), which is 3.7% higher than CNN and 3.1% higher than GNN. The model was tested on real seasonal data: in summer, solar irradiance reached  $800 \text{ W/m}^2$  with power output of 160 – 180 kW; in winter, it dropped to  $300 \text{ W/m}^2$ , with power output of 80 – 100 kW (Table 7). These results confirm that the model effectively adapts to climatic variations.
3. The model's efficiency and accuracy were evaluated.  $\text{MAE} \approx 1.75$  and  $\text{MSE} \approx 3.25$  were obtained, with 75% of residuals falling within the  $[-2, +2]$  range (Figure 8). The application of transfer learning improved forecasting accuracy by an average of 27% – 30%. For example, in the dry scenario, MAE decreased from 3.1 to 2.2. (Table 8). Moreover, with GPU (RTX 3060) acceleration, the computation time was reduced from 12.5 seconds to 4.3 seconds, increasing performance by 65.6% (Figure 9).

In conclusion, the proposed adaptive model demonstrates superior accuracy, seasonal adaptability, and computational efficiency compared to both traditional and modern methods. It is capable of providing reliable real-time forecasts under diverse climatic conditions and holds strong potential for integration into intelligent renewable energy management systems.

## References

- [1] Y. N. Zatsarinnaya, G. R. Valeeva, E. A. Shirobokov, M. M. Volkova, and D. R. Giniyatullina, "Prospects for Renewable Energy Development Until 2035," International Russian Automation Conference, pp. 382-392. Cham: Springer Nature Switzerland, 2024.
- [2] Q. Hassan *et al.*, "The renewable energy role in the global energy Transformations," *Renewable Energy Focus*, vol. 48, p. 100545, 2024. <https://doi.org/10.1016/j.ref.2024.100545>
- [3] A. Jäger-Waldau, "Snapshot of photovoltaics – February 2024," *EPJ Photovolt.*, vol. 15, p. 21, 2024. <https://doi.org/10.1051/epjpv/2024018>
- [4] V. H. U. Eze, E. Edozie, U. Kalyankolo, O. Okafor, C. N. Ugwu, and F. C. Ogenyi, "Overview of renewable energy power generation and conversion (2015-2023)," 2023.
- [5] M. Khaleel, Z. Yusupov, A. Ahmed, A. Alsharif, Y. Nassar, and H. El-Khozondar, "Towards sustainable renewable energy," *Applied Solar Energy*, vol. 59, no. 4, pp. 557-567, 2023. <https://doi.org/10.3103/S0003701X23600704>
- [6] L. D. O. Santos, T. AlSkaif, G. C. Barroso, and P. C. M. D. Carvalho, "Photovoltaic power estimation and forecast models integrating physics and machine learning: A review on hybrid techniques," *Solar Energy*, vol. 284, p. 113044, 2024. <https://doi.org/10.1016/j.solener.2024.113044>
- [7] M. Guermoui *et al.*, "An analysis of case studies for advancing photovoltaic power forecasting through multi-scale fusion techniques," *Scientific Reports*, vol. 14, no. 1, p. 6653, 2024. <https://doi.org/10.1038/s41598-024-57398-z>
- [8] K. J. Iheanetu, "Solar photovoltaic power forecasting: A review," *Sustainability*, vol. 14, no. 24, p. 17005, 2022. <https://doi.org/10.3390/su142417005>
- [9] J. Yu *et al.*, "Deep learning models for PV power forecasting: Review," *Energies*, vol. 17, no. 16, p. 3973, 2024. <https://doi.org/10.3390/en17163973>

- [10] G. Wu, Y. Wang, Q. Zhou, and Z. Zhang, "Enhanced photovoltaic power forecasting: An iTransformer and LSTM-based model integrating temporal and covariate interactions," in *2024 IEEE 8th Conference on Energy Internet and Energy System Integration (EI2)* (pp. 856-861). IEEE, 2024.
- [11] T. N. Nguyen and F. Müsgens, "What drives the accuracy of PV output forecasts?," *Applied Energy*, vol. 323, p. 119603, 2022. <https://doi.org/10.1016/j.apenergy.2022.119603>
- [12] G. Dai, S. Luo, H. Chen, and Y. Ji, "Efficient method for photovoltaic power generation forecasting based on state space modeling and BiTCN," *Sensors*, vol. 24, no. 20, p. 6590, 2024. <https://doi.org/10.3390/s24206590>
- [13] P. Di Leo, A. Ciocia, G. Malgaroli, and F. Spertino, "Advancements and challenges in photovoltaic power forecasting: A comprehensive review," *Energies*, vol. 18, no. 8, p. 2108, 2025. <https://doi.org/10.3390/en18082108>
- [14] C. Zhang, Y. Zhang, C. Hu, Z. Liu, L. Cheng, and Y. Zhou, "A novel intelligent fault diagnosis method based on variational mode decomposition and ensemble deep belief network," *IEEE Access*, vol. 8, pp. 36293-36312, 2020. <https://doi.org/10.1109/ACCESS.2020.2969412>
- [15] X. Luo and D. Zhang, "An adaptive deep learning framework for day-ahead forecasting of photovoltaic power generation," *Sustainable Energy Technologies and Assessments*, vol. 52, p. 102326, 2022. <https://doi.org/10.1016/j.seta.2022.102326>
- [16] A. Li, B. Su, and J. Young, "Photovoltaic power generation prediction via pre-training Mamba. Tsinghua University Course: Advanced Machine Learning," 2024. <https://openreview.net/forum?id=qHvMPEMkGU>
- [17] A. K. Bansal, "Sizing and forecasting techniques in photovoltaic-wind based hybrid renewable energy system: A review," *Journal of Cleaner Production*, vol. 369, p. 133376, 2022. <https://doi.org/10.1016/j.jclepro.2022.133376>
- [18] A. Kuttybayeva, A. Abdykadyrov, G. Tolen, A. Burdin, V. Malyugin, and D. Kiesewetter, "Development and optimization of distributed acoustic sensors for seismic monitoring," in *2024 International Conference on Electrical Engineering and Photonics (EExPolytech)* (pp. 64-67). IEEE, 2024.
- [19] A. Kuttybayeva, A. Abdykadyrov, G. Tolen, A. Burdin, V. Malyugin, and D. Kiesewetter, "Application of distributed acoustic sensors based on optical fiber technologies for infrastructure monitoring," in *2024 International Conference on Electrical Engineering and Photonics (EExPolytech)* (pp. 23-26). IEEE, 2024.
- [20] A. Abdykadyrov, S. Marxuly, G. Tolen, A. Kuttybayeva, M. Abdullayev, and G. Sharipova, "Optimization of data transmission in sensor networks for enhanced control of ozonator efficiency," *Eastern-European Journal of Enterprise Technologies*, vol. 6, no. 2 (132), pp. 83-94, 2024. <https://doi.org/10.15587/1729-4061.2024.318585>
- [21] S. Marxuly, A. Abdykadyrov, K. Chezhibayeva, and N. Smailov, "Study of the ozone control process using electronic sensors," *Informatyka, Automatyka, Pomiary w Gospodarce i Ochronie Środowiska*, vol. 14, no. 4, pp. 38-45, 2024. <https://doi.org/10.35784/iapgos.6051>
- [22] A. Abdykadyrov et al., "Optimization of distributed acoustic sensors based on fiber optic technologies," *Eastern-European Journal of Enterprise Technologies*, vol. 5, no. 5 (131), pp. 50-59, 2024. <https://doi.org/10.15587/1729-4061.2024.313455>
- [23] N. Smailov et al., "Streamlining digital correlation-interferometric direction finding with spatial analytical signal," *Informatyka, Automatyka, Pomiary w Gospodarce i Ochronie Środowiska*, vol. 14, no. 3, pp. 43-48, 2024. <https://doi.org/10.35784/iapgos.6177>
- [24] A. Sabibolda, V. Tsymporenko, N. Smailov, V. Tsymporenko, and A. Abdykadyrov, "Estimation of the time efficiency of a radio direction finder operating on the basis of a searchless spectral method of dispersion-correlation radio direction finding," *IFTToMM Asian conference on Mechanism and Machine Science* (pp. 62-70). Cham: Springer Nature Switzerland, 2024.
- [25] N. Smailov et al., "Improving the accuracy of a digital spectral correlation-interferometric method of direction finding with analytical signal reconstruction for processing an incomplete spectrum of the signal," *Eastern-European Journal of Enterprise Technologies*, vol. 5, no. 9 (125), pp. 14-25, 2023. <https://doi.org/10.15587/1729-4061.2023.288397>
- [26] A. Sabibolda et al., "Improving the accuracy and performance speed of the digital spectral-correlation method for measuring delay in radio signals and direction finding," *Eastern-European Journal of Enterprise Technologies*, vol. 1, no. 9(115), pp. 6-14, 2022. <https://doi.org/10.15587/1729-4061.2022.252561>